Atmos. Chem. Phys. Discuss., 14, 23681–23709, 2014
www.atmos-chem-phys-discuss.net/14/23681/2014/
doi:10.5194/acpd-14-23681-2014

Atmospheric Chemistry and Physics Discussions

The potential for regional-scale bias in top-down CO_2 flux estimates due to atmospheric transport errors

S. M. Miller[1], I. Fung[2], J. Liu[3], M. N. Hayek[1], and A. E. Andrews[4]

[1]Department of Earth and Planetary Sciences, Harvard University, Cambridge, MA, USA
[2]Department of Earth and Planetary Sciences, University of California–Berkeley, Berkeley, CA, USA
[3]Earth Science Division, Jet Propulsion Laboratory, NASA, Pasadena, CA, USA
[4]Global Monitoring Division, Earth Systems Research Laboratory, National Oceanic and Atmospheric Administration, Boulder, CO, USA

Received: 18 August 2014 – Accepted: 19 August 2014 – Published: 15 September 2014

Correspondence to: S. M. Miller (scot.m.miller@gmail.com)

Published by Copernicus Publications on behalf of the European Geosciences Union.

Abstract

Estimates of CO_2 fluxes that are based on atmospheric data rely upon a meteorological model to simulate atmospheric CO_2 transport. These models provide a quantitative link between surface fluxes of CO_2 and atmospheric measurements taken downwind. Therefore, any errors in the meteorological model can propagate into atmospheric CO_2 transport and ultimately bias the estimated CO_2 fluxes. These errors, however, have traditionally been difficult to characterize. To examine the effects of CO_2 transport errors on estimated CO_2 fluxes, we use a global meteorological model-data assimilation system known as "CAM–LETKF" to quantify two aspects of the transport errors: error variances (standard deviations) and temporal error correlations. Furthermore, we develop two case studies. In the first case study, we examine the extent to which CO_2 transport uncertainties can bias CO_2 flux estimates. In particular, we use a common flux estimate known as CarbonTracker to discover the minimum hypothetical bias that can be detected above the CO_2 transport uncertainties. In the second case study, we then investigate which meteorological conditions may contribute to month-long biases in modeled atmospheric transport.

We estimate 6 hourly CO_2 transport uncertainties in the model surface layer that range from 0.15 to 9.6 ppm (standard deviation), depending on location, and we estimate an average error decorrelation time of ~ 2.3 days at existing CO_2 observation sites. As a consequence of these uncertainties, we find that CarbonTracker CO_2 fluxes would need to be biased by at least 29 %, on average, before that bias were detectable at existing non-marine atmospheric CO_2 observation sites. Furthermore, we find that persistent, bias-type errors in atmospheric transport are associated with consistent low net radiation, low energy boundary layer conditions. The meteorological model is not necessarily more uncertain in these conditions. Rather, the extent to which meteorological uncertainties manifest as persistent atmospheric transport biases appears to depend, at least in part, on the energy and stability of the boundary layer. Existing

CO_2 flux studies may be more likely to estimate inaccurate regional fluxes under those conditions.

1 Introduction

Scientists increasingly use atmospheric CO_2 observations to estimate CO_2 fluxes at the Earth's surface (e.g., Gurney et al., 2002; Michalak et al., 2004; Peters et al., 2007; Gourdji et al., 2012). This "top-down" approach contrasts with "bottom-up" studies that rely primarily on expert knowledge of biological processes (e.g., Huntzinger et al., 2012; Raczka et al., 2013). In order to estimate the fluxes, top-down studies typically require a meteorology model to link fluxes at the surface with measurements taken downwind. Using this link, one can estimate the fluxes even if the atmospheric measurements do not themselves directly measure the fluxes.

However, both the accuracy and effective resolution of the flux estimate hinge upon the accuracy of the meteorological model. Errors in the meteorological model may (or may not) translate into errors in CO_2 transport from the location(s) of surface fluxes to the atmospheric measurement site(s). Subsequently, errors in CO_2 transport may (or may not) bias estimated CO_2 fluxes depending upon the error characteristics and the space/time scales of interest. This cascading chain of cause and effect defines the three types of errors or uncertainties that are of primary interest in this paper: (1) errors in modeled meteorological variables, (2) errors in atmospheric CO_2 transport, as they manifest in modeled atmospheric CO_2 concentrations, and (3) errors in the fluxes that result from problems in estimated transport. This study is particularly concerned with how CO_2 transport errors may propagate into the estimated fluxes.

More specifically, the effect of CO_2 transport errors on the estimated fluxes depends upon two important factors. First, the flux estimate becomes more uncertain as the CO_2 transport error variance (or standard deviation) increases. Top-down studies that use Bayesian statistics will explicitly account for these variances when estimating fluxes (e.g., Enting, 2002; Tarantola, 2005); before estimating the fluxes, the modeler first

estimates the total variance due to an array of model or data errors – due to imperfect atmospheric transport or imperfect measurements, among many other sources of error (e.g. Gerbig et al., 2003; Michalak et al., 2005; Ciais et al., 2011).

Second, the flux estimate becomes more uncertain as the temporal and/or spatial covariance in the errors increases. As the covariances increase, each CO_2 measurement effectively provides less and less independent information to constrain the surface fluxes. Error correlations, however, are often difficult to characterize (e.g. Lin and Gerbig, 2005; Lauvaux et al., 2009) and are omitted from most existing top-down studies. These difficulties aside, correlated transport errors can have a number of impacts on the estimated greenhouse gas fluxes. First, a top-down study that does not account for these errors will typically underestimate the uncertainties in the flux estimate. Second, correlated errors can bias the flux estimate over a region or over the entire geographic area of interest (e.g., Stephens et al., 2007).

Quantification of this complex cause-and-effect between meteorological errors and errors in estimated CO_2 fluxes represents an ongoing research challenge, and a number of existing studies have partly characterized these uncertainties. For example, a series of studies known as "TRANSCOM" represents one of the first coordinated projects on CO_2 transport uncertainties (Gurney et al., 2002; Baker et al., 2006). These early studies used 13 different global atmospheric models and compared differences in top-down CO_2 budgets due to atmospheric model differences. These models gave an uncertainty in the Northern Hemisphere CO_2 budget of $\pm 1.1\,\mathrm{Pg\,C\,yr^{-1}}$ (standard deviation; mean budget of $2.4\,\mathrm{Pg\,C\,yr^{-1}}$) (Stephens et al., 2007). Subsequent to the TRANSCOM project, a number of studies have focused on the effects of changing vertical mixing and/or planetary boundary layer height (PBLH) (Gerbig et al., 2008; Kretschmer et al., 2012, 2014; Parazoo et al., 2012; Pino et al., 2012). In general, these papers found that uncertainties in PBLH can lead to errors of up to ~ 3 ppm in modeled CO_2. Another paper examined the effect of uncertain horizontal winds (Lin and Gerbig, 2005). The authors applied a particle-trajectory model at a measurement site in Wisconsin and found that uncertainties in the horizontal winds contributed ~ 6 ppm (standard de-

viation) to the overall CO_2 transport uncertainty. In summary, a number of previous studies have either perturbed individual meteorological parameters or, in the case of TRANSCOM, sampled a subset of transport uncertainties using 13 pre-selected atmospheric models.

Numerous questions still remain, however. For example, if one could carefully utilize all available meteorological observations, what meteorological and CO_2 transport uncertainties would remain? Furthermore, what is the combined effect of meteorological errors from multiple parameters (e.g., wind, boundary layer, etc.) on CO_2 transport and subsequently on CO_2 fluxes? In addition, which meteorological errors are most likely to bias regional-scale CO_2 flux estimates on month-long time scales?

In the present study, we explore several facets of these questions using a global meteorology model ensemble and a meteorology data assimilation system – the Community Atmosphere Model (CAM) and an assimilation framework known as a Local Ensemble Transform Kalman Filter (LETKF) (Hunt et al., 2007; Liu et al., 2011). CAM–LETKF systematically estimates meteorology and CO_2 transport uncertainties to an extent not previously possible; this framework explicitly represents the CO_2 transport uncertainties that remain after assimilating several hundred thousand meteorology observations at each 6 h model time step. To accomplish this task, CAM–LETKF uses an ensemble of weather forecasts and optimizes the ensemble to match available meteorological observations. Furthermore, CAM-LETKF adjusts the variance of the weather ensemble at each time step to match the modeling uncertainties implied by the meteorological observations.

Using this toolkit, we construct two case studies to understand both the possible magnitude and potential drivers of bias in top-down CO_2 flux budgets. Previous studies by Liu et al. (2011) and Liu et al. (2012) used CAM–LETKF to estimate CO_2 transport uncertainties, and this study investigates connections with top-down CO_2 flux estimation. First, we construct a case study with a commonly-used estimate of CO_2 fluxes known as CarbonTracker (CT): how biased would regional CO_2 fluxes need to be before that bias were detectable above the meteorological uncertainties estimated by

CAM–LETKF? We test this hypothesis at a number of atmospheric CO_2 monitoring sites in the US, Canada, Europe, and East Asia. Second, we construct a case study using a synthetic atmospheric tracer. This synthetic experiment serves as a lens to explore the possible meteorological factors associated with persistent, month-long deviations in atmospheric transport.

2 Methods

2.1 The meteorology and CO_2 model

The first component of CAM–LETKF is the meteorological model. We simulate global meteorology using the Community Atmosphere Model (CAM) and Community Land Model (CLM, version 3.5), run in weather forecast mode (not climate mode) (Collins et al., 2006; Oleson et al., 2008; Chen et al., 2010). Model simulations in this study have a spatial resolution of 2.5° longitude by 1.9° latitude with 26 vertical model levels. We save the global model output at 6 h time increments. Furthermore, we run the model for two time periods: January–February 2009 and May–July 2009. The first month of each run serves as an initial spin-up for the model-data assimilation system. The next section describes this assimilation in greater detail.

2.2 The meteorological model-data assimilation framework

The second component of CAM–LETKF is the data assimilation and model optimization framework. This framework serves two purposes. First, the LETKF optimizes modeled meteorology (CAM–CLM) to match available observations. Second, the LETKF uses an ensemble of model forecasts to represent model uncertainties that remain after data assimilation (Hunt et al., 2004, 2007). We define each ensemble member and the mean of the entire ensemble as follows:

$$\boldsymbol{x}_i = \bar{\boldsymbol{x}} + \mathbf{X}_i \quad \text{where } i = 1 \ldots k \tag{1}$$

where $\boldsymbol{x}_i$ ($m_1 \times 1$) is a single model ensemble member, $\bar{\boldsymbol{x}}$ ($m_1 \times 1$) is the mean of the model ensemble, and $\mathbf{X}_i$ ($m_1 \times k$) refers to the ith column of the matrix that defines the ensemble spread. In this paper, the variable m_1 refers to the total number of model parameters – the model estimate for a variety of meteorological variables, concatenated across the globe and across all 6 hourly time steps in a given model run. Furthermore, we use $k = 64$ total ensemble members in this setup, as was done in Liu et al. (2011) and Liu et al. (2012).

Using this ensemble, CAM–LETKF steps through time in sequential 6 h intervals. First, the model ensemble at time t is optimized to match meteorological data. To this end, we assimilate the same meteorological observations used in the National Centers for Environmental Prediction-Department of Energy reanalysis 2 (Kanamitsu et al., 2002): temperature (in situ and satellite), zonal wind (in situ and satellite), meridional wind (in situ and satellite), surface pressure (in situ), and specific humidity (in situ). At each 6 h model time step, we assimilate between ~ 180 000 to 330 000 observations globally. At that juncture, the ensemble mean associated with time t, $\bar{\boldsymbol{x}}(t)$, represents the model best guess and the ensemble members, $\bar{\boldsymbol{x}}(t) + \mathbf{X}(t)$, collectively represent the posterior variances and covariances in the modeled meteorology. For the remainder of this paper, we define the 6 hourly meteorological uncertainties as the standard deviation (or alternately, the range) of each row in $\mathbf{X}$. Second, we run 6 h CAM–CLM forecasts using these realizations as initial conditions – a total of 64 model forecasts. This ensemble of global forecasts then becomes the prior (and prior variances and covariances) for the next LETKF assimilation cycle (Hunt et al., 2007). The 6 h cycle of data assimilation and model forecast then begins again.

This model ensemble, by design, is guaranteed to reflect actual uncertainties in modeled meteorology; at each 6 h model time step, we adjust the ensemble variance such that this variance matches against the model–data residuals (Li et al., 2009; Miyoshi, 2011). The Supplement describes this procedure, known as adaptive covariance inflation. For further technical detail on the LETKF and adaptive covariance inflation, refer

to the Supplement, Hunt et al. (2004), Hunt et al. (2007), Li et al. (2009), Liu et al. (2011), or Miyoshi (2011).

2.3 CO_2 transport error variances and covariances

The CAM–LETKF system described above estimates not only meteorological uncertainties but also uncertainties in CO_2 transport. In this study, CO_2 is a passive tracer and is not part of the data assimilation. Instead, we use biospheric, oceanic, biomass burning, and fossil fuel CO_2 fluxes from CT (version "CT2011_oi", Fig. 1) (Peters et al., 2007, http://carbontracker.noaa.gov). Furthermore, we use CT as the initial condition for global atmospheric CO_2 mixing ratios on 1 January and 1 May 2009. Each CAM ensemble member uses the same initial condition for atmospheric CO_2, so any subsequent differences in CO_2 among the model realizations are due entirely to meteorological uncertainties.

We estimate 6 hourly CO_2 transport uncertainties using the standard deviation of CO_2 concentrations across the 64 model realizations (e.g., Fig. 2). To make this estimate, we calculate the standard deviation of each row in $\mathbf{X}_{[CO_2]}$, where the subscript "$[CO_2]$" refers to the atmospheric CO_2 concentrations estimated by the ensemble. In addition, we characterize temporal covariance or correlation in transport errors (i.e., in $\mathbf{X}_{[CO_2]}$). To estimate an error decorrelation time, we use a variogram analysis. In specific, we fit an exponential variogram model to afternoon-only model output (1–7 p.m. LT) associated with a number of existing, global atmospheric CO_2 observation sites. Both Kitanidis (1997) and the Supplement describe variograms in greater detail. The remainder of the methods section applies this CO_2 and meteorology modeling framework to two case studies.

2.4 Case study 1: how biased would CarbonTracker fluxes need to be before that bias were detectable above CO_2 transport uncertainties?

In this case study, we construct a hypothesis test to determine whether biases in CT CO_2 fluxes would be detectable above atmospheric transport uncertainties. CT is a commonly-used global CO_2 flux estimate created by the US National Oceanic and Atmospheric Administration (NOAA). To create CT, NOAA scientists use atmospheric CO_2 data from observations towers and surface sites around the world and estimate regional scaling factors that optimize an initial CO_2 flux model (Peters et al., 2007).

We test whether a hypothetical bias in regional scaling factors, like those estimated by CT, would be detectable at atmospheric CO_2 observation sites across the globe. We build this test using the CO_2 sum of squared residuals (SSR) from the CAM–LETKF model ensemble. A number of previous statistical and/or greenhouse gas studies construct hypothesis tests using squared residuals (e.g., Sheskin, 2003; Huntzinger et al., 2011).

In this setup, we construct the test as follows. First, compute the SSR associated with the transport uncertainties:

$$\mathrm{SSR} = \sum^{n_2} \left(\mathbf{H}_{[\mathrm{CO}_2]} \mathbf{X}_{[\mathrm{CO}_2]} \right)^2 \tag{2}$$

This equation interpolates the model residuals ($\mathbf{X}_{[\mathrm{CO}_2]}$) to the observation sites, squares these residuals, and sums them over the entire time period of interest. More specifically, the variable n_2 refers to the number of hourly CO_2 observations at an observation site over the time span of the hypothesis test. In addition, $\mathbf{H}_{[\mathrm{CO}_2]}$ ($n_2 \times m_2$) is the matrix that interpolates or maps the ensemble deviations ($\mathbf{X}_{[\mathrm{CO}_2]}$, dimensions $m_2 \times k$) to the CO_2 observations. Lastly, SSR ($1 \times k$) are the sum of squared residuals from each of the k CAM–LETKF model ensemble members. Note that some of the ensemble members will be closer than others to the ensemble mean or best estimate ($\bar{\boldsymbol{x}}_{[\mathrm{CO}_2]}$). Therefore, the k SSRs from the k ensemble members will not be identical and will instead form a distribution.

Second, we compute the SSR associated with a hypothetical bias (λ) in the fluxes:

$$\mathrm{FSSR} = \sum^{n_2} (\Delta \mathrm{CO}_2)^2$$

$$\Delta \mathrm{CO}_2 = \lambda \mathbf{H}_{[\mathrm{CO}_2]} \left(\bar{\boldsymbol{x}}_{[\mathrm{CO}_2,\mathrm{surface}]} - \bar{\boldsymbol{x}}_{[\mathrm{CO}_2,600\,\mathrm{hPa}]} \right) \tag{3}$$

The output of this equation, FSSR, is a scalar that estimates the squared residuals due to a biased flux estimate, summed over all observations at a given CO_2 measurement site. The variable λ represents a hypothetical bias in CT fluxes. In this study, we conduct the hypothesis test at each measurement site individually, so the variable λ is specific to the site being considered. In addition, the variables in parentheses ($\bar{\boldsymbol{x}}_{[\mathrm{CO}_2,\mathrm{surface}]} - \bar{\boldsymbol{x}}_{[\mathrm{CO}_2,600\,\mathrm{hPa}]}$) quantify the contribution of regional-scale fluxes to CO_2 at the atmospheric observation site. Many top-down studies pre-subtract free troposphere or marine "clean air" concentrations from the CO_2 measurements or model output at the observation sites (e.g., Gerbig et al., 2003; Gourdji et al., 2012). These top-down studies then optimize regional fluxes to match the pre-subtracted CO_2 observations. In this study, we similarly subtract modeled concentrations at 600 hPa in the free troposphere ($\bar{\boldsymbol{x}}_{[\mathrm{CO}_2,600\,\mathrm{hPa}]}$) from those at the CO_2 observation sites ($\bar{\boldsymbol{x}}_{[\mathrm{CO}_2,\mathrm{surface}]}$). The concentrations at 600 hPa are not necessarily a perfect measure of "clean air" concentrations. Rather, this approach is an approximation similar to that used in the existing literature. This difference in concentrations is then used to estimate how a regional bias in CT fluxes would manifest at a given observation site (ΔCO_2, in ppm).

Finally, we test the hypothesis. If the FSSR is larger than most of the k SSR associated with the meteorological uncertainties, then we can distinguish the flux bias (λ) above the meteorological noise. This statement can be formalized into a hypothesis test as follows:

$$A = \{\mathrm{SSR} \mid \mathrm{SSR} > \mathrm{FSSR}\} \tag{4}$$

$$p = \frac{|A|}{k} \tag{5}$$

where A is the set of SSR that are greater than FSSR, and the expression $|A|$ indicates the number of elements in A. If the p value is less than 0.05, we have disproven the null hypothesis – that the hypothetical bias (λ) in CO_2 fluxes is indistinguishable above the transport uncertainties.

Note that this hypothesis test accounts for both variance and temporal covariance in the CO_2 transport uncertainties, a concept discussed in detail in the Supplement. In addition, note that FSSR will almost never be zero due to diurnal or daily changes in NEP, even if the monthly-averaged NEP at a given site is zero.

We conduct the hypothesis test above for both February and July 2009 at a variety of different observation sites in North America, Asia, and Europe. We report the results of this hypothesis test for a representative selection of global CO_2 observation sites – different types of observation towers located on different continents and in different biomes. Furthermore, we test this hypothesis using month-long modeled time series corresponding to afternoon data only (1–7 p.m. LT). We use this month-long window because CO_2 budgets are often reported in month-long increments.

In summary, case study 1 quantifies the extent to which atmospheric CO_2 transport errors can obscure any regional biases in estimated CO_2 fluxes. The next case study, in contrast, explores the meteorological conditions under which sustained CO_2 transport errors may be more likely to occur.

2.5 Case study 2: which meteorological factors may be associated with sustained, month-long transport biases?

We create a relatively simple, synthetic experiment to explore the meteorological conditions under which month-long model biases in atmospheric transport may occur. The spatial patterns in the CO_2 transport uncertainties are heavily influenced by spatial patterns in the CO_2 fluxes (Fig. 2). In other words, regions with large fluxes or large diurnal flux variability also show higher CO_2 transport uncertainties. As a result, it is difficult to disentangle the effect of different meteorological parameters on CO_2 transport uncertainties. Instead, we create a synthetic tracer with constant global emissions in both

space and time. This experiment serves as a lens to explore the possible effects of different meteorological parameters independent of the spatial variability in CO_2 fluxes.

To this end, we initialize CAM-LETKF runs with zero atmospheric concentration of this synthetic tracer and then run CAM-LETKF forward for one month using constant global emissions (e.g., for both February and July 2009). Any uncertainties in the atmospheric distribution of this tracer are solely due to meteorological parameters, not due to the spatial distribution of the underlying fluxes.

Next, we calculate the coefficient of variation (CV) associated with the monthly-averaged surface concentrations. The CV is an inverted signal-to-noise ratio; it measures the uncertainty in modeled surface concentrations relative to the average surface concentration ($\frac{\sigma}{\mu}$). For example, an uncertainty of 1 ppm in modeled concentrations is most problematic if the signal from surface fluxes is weak, and a 1 ppm uncertainty is less problematic if the signal from surface sources is strong.

For this setup, the CV equals the standard deviation in the monthly-averaged surface concentrations divided by the monthly surface concentration averaged across all 64-realizations. We then plot the tracer CV against monthly-averaged meteorological parameters and their associated uncertainties from CAM–LETKF. These relationships give insight into the meteorological conditions or meteorological uncertainties that are associated with month-long biases in the modeled synthetic tracer.

3 Results and discussion

3.1 Uncertainties in the 6 hourly modeled CO_2 concentrations

Before examining the two case studies in detail, we first provide context on the CO_2 transport uncertainties estimated with CT fluxes and CAM–LETKF. Figure 2a and b visually summarize the average 6 hourly CO_2 transport uncertainties (standard deviations) in the model surface layer; these figures show how CO_2 transport uncertainties vary across the globe – from 0.15 to 9.6 ppm (standard deviation), depending on loca-

tion. Furthermore, the transport uncertainties in Fig. 2a and b show several distinctive features. The largest uncertainties are localized to regions where either the magnitude or the diurnal cycle of the CT fluxes is largest (e.g., the US Eastern Seaboard and southern Siberia during summertime, the Amazon, the Congo, and eastern China). CO_2 transport uncertainties in the Eastern US and East Asia bleed, to a smaller degree, over the adjacent ocean where surface fluxes are small.

These transport uncertainties are in the range of the uncertainties estimated in a number of previous studies. For example, the spatial patterns in the 6 hourly uncertainties are similar to those modeled by Liu et al. (2011) using CAM-LETKF and temperature-scaled CO_2 fluxes from TRANSCOM 3. In addition, a number of previous studies focused on the effects of perturbing individual meteorological parameters at specific observation sites or for individual aircraft campaigns (e.g., Gerbig et al., 2003, 2008; Lin and Gerbig, 2005; Kretschmer et al., 2012). Our 6 hourly transport uncertainties, though very different in both scope and scale, are comparable in magnitude to the individual parameter uncertainties estimated by Gerbig et al. (2003), Gerbig et al. (2008), and Kretschmer et al. (2012) but are less than the uncertainties in Lin and Gerbig (2005). Furthermore, our estimated 6 hourly transport uncertainties also appear similar to or slightly smaller than the model–data mismatch errors estimated at individual observation sites in several inversion studies (e.g., Peters et al., 2007; Schuh et al., 2010; Gourdji et al., 2012). Model–data mismatch includes not only transport errors but also any model or data errors unrelated to an imperfect initial flux estimate. This result may reflect the fact that atmospheric transport often dominates model-data mismatch errors.

Figure 3 places these transport uncertainties in context of CO_2 data measured at two observation sites in the United States. These time series plots validate the model's capacity to simulate daily variations in CO_2 concentrations. Furthermore, the comparison illustrates the magnitude of the CO_2 transport uncertainties relative to the diurnal cycle in CO_2 concentrations. For example, the uncertainties at AMT in July are $\sim 30\,\%$ of the diurnal range in the CO_2 measurements. Overall, the model ensemble depicted

in these plots usually encapsulates the hourly-averaged measurements. CT fluxes are estimated using these CO_2 observations and the TM5 transport model (Tracer Model, version 5) (Peters et al., 2007), so one might expect the CAM model to fit the CO_2 observations relatively well. In the instances when the model ensemble does not encapsulate the hourly-averaged CO_2 measurements, one of the many other non-transport error types could be to blame; the ensemble spread only encompasses transport error and does not include measurement error, error due to finite model resolution, or errors in the fluxes. The Supplement provides more example CO_2 model–data comparisons, meteorology model validation, and data assimilation diagnostics.

3.2 CO_2 transport uncertainties at longer time scales

The uncertainty in monthly-averaged CO_2 concentrations provides one measure of how transport errors persist over time. In other words, these uncertainties provide a metric of error correlations in CO_2 transport. Uncorrelated transport errors will average out, to a large degree, over many model time steps, but temporal correlations prevent the errors from averaging down over time. As a result, large uncertainties in monthly-averaged concentrations indicate the potential for persistent bias in CO_2 fluxes estimated using atmospheric observations. Such bias could lead to under- or over-estimation of regional-scale CO_2 budgets.

To this end, Fig. 2c and d displays uncertainties in the month-long average surface concentrations for February and July 2009. In contrast to the 6 hourly uncertainties, these uncertainties are far more spatially-distributed; the largest uncertainties are not just associated with regions that have large fluxes. This result implies that CO_2 transport errors are correlated over longer periods of time in remote regions, compared to regions with large anthropogenic or biospheric fluxes. Furthermore, month-long transport uncertainties are large across the entire Northern Hemisphere during February even though biospheric fluxes are weak during that time period. A subsequent Sect. 3.4 explores possible reasons why these month-long biases occur. In particular, the case

study discussed in that section provides insight into why the month-long uncertainties may be large across the Northern Hemisphere during winter.

A variogram analysis provides an additional measure of the error correlations in CO_2 transport (see Sect. 2.3 and the Supplement). Based upon this analysis, we estimate CO_2 transport error decorrelation times of 2.2 and 2.3 days at global atmospheric CO_2 observation sites during February and July, respectively (see Table S1). The error decorrelation times are generally longer at marine sites (average of 2.9 and 2.7 days in February and July, respectively) or at sites that are far from large CO_2 fluxes. For example, the longest error decorrelation times occur at coastal sites in Japan, Korea and the Canary Islands. In contrast, decorrelation times are usually shorter than average for observation sites on the European mainland.

This level of temporal correlation in the CO_2 transport errors implies several large-scale conclusions for estimating CO_2 fluxes. First, observation sites that are far from large fluxes are more likely to produce a biased CO_2 budget than sites near to large surface fluxes. These "remote" sites see a lower CO_2 signal from surface fluxes, and the transport errors at these locations are generally correlated over longer periods of time. Second, most existing top-down studies will underestimate the uncertainties in estimated CO_2 fluxes. Existing inversions rarely account for error correlations in CO_2 transport and most likely underestimate the posterior uncertainties as a direct result. The next Sect. 3.3 quantifies the impact of the transport uncertainties discussed above on surface flux estimation.

3.3 Case study 1: how biased would CT fluxes need to be before that bias were detectable above the CO_2 transport uncertainties?

We use a case study from CT to understand how transport errors translate into uncertainty in a top-down, CO_2 flux estimate. In specific, if the flux scaling factors estimated by CT were incorrect, how wrong would those scaling factors need to be before the problem were detectable above atmospheric transport errors?

Figure 4 shows the results of this case study (described in Sect. 2.4) at a selection of global CO_2 observation sites. The y-axis of each bar plot shows the minimum bias that would be detectable using hourly-averaged CO_2 observations collected over an entire month. The mean minimum detectable bias across all non-marine sites is 29 % (at a month-long time scale). The results are not substantially different at short versus tall non-marine tower sites: 27 % and 31 %, respectively. In other words, the tall towers examined in this analysis are neither more or less sensitive to biased CO_2 fluxes in comparison to the set of short towers in Fig. 4. At marine sites, in contrast, the minimum detectable bias is far larger: 76 % on average.

These results show a number of additional trends across the different observation sites. In general, towers that are near large sources are better able to detect bias in the modeled fluxes. These include observation sites in the central and eastern US or in Germany and Eastern Europe – sites that are strongly influence by terrestrial (versus marine) airflow relative to other locations. Most of these towers see large signals from biospheric fluxes during summer (Figs. S9–S14). Other towers, in contrast, are less sensitive to detecting bias during the summertime (e.g., the marine towers and towers in the western US). The western US towers, for example, are surrounded by weak biosphere uptake that is diluted into a larger mixed layer during summer. But during summer, transport uncertainties increase due to large seasonal fluxes in adjacent regions. The sensitivity of the marine Japanese and Korean sites also declines in the summer. At these sites, the signal from surface fluxes is largest in winter. During summer, biosphere uptake somewhat cancels the signal from large anthropogenic emissions in China.

Note that this analysis only considers uncertainties due to meteorology. The capabilities of the atmospheric observations would deteriorate if other errors were included (e.g., measurement errors or errors due to model resolution).

3.4 Case study 2: which meteorological factors are associated with sustained, month-long atmospheric transport biases?

We now examine the results of the synthetic tracer experiment (Sect. 2.5) to uncover possible drivers of atmospheric transport biases.

Figure 5 displays the coefficient of variation (CV) for monthly-averaged surface concentrations of the synthetic tracer. The CV, a unitless quantity, does not just indicate where the uncertainties are largest. Rather, the CV indicates the magnitude of these uncertainties relative to the mean modeled tracer concentration. Arguably, this noise-to-signal ratio measures the influence of transport uncertainties more effectively than a simple standard deviation. The remainder of this section focuses only on land regions because most existing top-down studies focus on land fluxes.

This coefficient shows a number of distinctive seasonal and spatial patterns. Like the uncertainties in monthly-averaged CO_2 (Fig. 2c and d), the CV in Fig. 5 is highest in boreal and arctic regions of the Northern Hemisphere during winter. The CV is lowest over Europe, Australia, and the Amazon during all seasons.

We plot the synthetic tracer CV against numerous modeled meteorological parameters to understand the possible drivers behind the transport uncertainties. Of the 60 variables tested (Table S2), seven of the variables showed correlations (R^2) with the tracer CV that are greater or equal to 0.3 (Fig. 6). Meteorological conditions that lead to high atmospheric stability and low energy are most closely associated with persistent tracer uncertainties (relative to mean surface concentrations). For example, a high tracer CV is associated with low temperatures, low net radiative flux, low net solar flux, low planetary boundary layer height, and low vertical diffusion diffusivity. Furthermore, many of the meteorological variables exhibit a nonlinear relationship with the tracer CV; the CV increases more quickly when net radiation and planetary boundary heights are low.

The results of this synthetic tracer experiment hold a number of potential applications to top-down CO_2 flux estimation. The danger of obtaining a biased CO_2 budget is likely

higher in regions with consistent low energy, limited vertical mixing, and/or high albedo. These biases are unlikely to be represented by most existing inversion uncertainty calculations, as explained in the previous sections. Furthermore, the meteorological model ensemble is not necessarily more uncertain these regions (see Figs. S16 and S17). Note that month-long CO_2 transport biases did not correlate as strongly with meteorology uncertainties. Rather, the extent to which meteorological uncertainties translate into tracer transport uncertainties appears to depend, at least in part, on the stability and net energy input associated with the boundary layer.

4 Conclusions

In this paper, we use two case studies to investigate the potential for bias in top-down CO_2 flux estimates due to errors in modeled atmospheric CO_2 transport. The first case study examines the ability of in situ atmospheric observations to detect bias in estimated CO_2 fluxes. Among other results, we find that CT would need to be biased by 29 %, on average, before that bias were detectable above CO_2 transport uncertainties at terrestrial, atmospheric observation sites. These results are strongly influenced by temporal correlations in the transport uncertainties. In other words, atmospheric CO_2 measurements contain less information about the fluxes than is usually assumed by top-down studies that overlook transport error covariances. As a result, most existing inversions are likely to underestimate the uncertainties in estimated CO_2 fluxes and/or may be vulnerable to unforeseen biases in the estimated fluxes. Accounting for these correlated errors can be as simple as modifying one of the covariance matrix inputs in a Bayesian inversion. Accordingly, this study provides information to improve the setup of future top-down inverse modeling studies – an improvement that will widen the confidence interval on the estimated fluxes.

In a subsequent case study, we investigate the factors associated with month-long biases in atmospheric transport. The largest short-term CO_2 transport errors correlate strongly with the location of the largest surface fluxes, but month-long biases in at-

mospheric transport are not only localized to regions with large fluxes. Rather, these biases may be more likely to occur at observation sites that are far from large fluxes and in regions with high atmospheric stability and low net radiation. Existing top-down flux studies may be more likely to estimate inaccurate regional fluxes under those conditions.

The Supplement related to this article is available online at doi:10.5194/acpd-14-23681-2014-supplement.

Acknowledgements. This work was conducted at the Department of Energy's (DOE) Lawrence Berkeley National Laboratory as part of a DOE Computational Science Graduate Fellowship. The research used resources of the National Energy Research Scientific Computing Center, which is supported by the DOE's Office of Science under Contract No. DE-AC02-05CH11231. CarbonTracker CT2011_oi results are provided by NOAA ESRL, Boulder, Colorado, USA from the website at http://carbontracker.noaa.gov. We thank Steven Wofsy for his feedback on the manuscript and thank Ed Dlugokencky of NOAA.

References

Baker, D. F., Law, R. M., Gurney, K. R., Rayner, P., Peylin, P., Denning, A. S., Bousquet, P., Bruhwiler, L., Chen, Y.-H., Ciais, P., Fung, I. Y., Heimann, M., John, J., Maki, T., Maksyutov, S., Masarie, K., Prather, M., Pak, B., Taguchi, S., and Zhu, Z.: TransCom 3 inversion intercomparison: impact of transport model errors on the interannual variability of regional CO_2 fluxes, 1988–2003, Global Biogeochem. Cy., 20, GB1002, doi:10.1029/2004GB002439, 2006. 23684

Chen, H., Zhou, T., Neale, R. B., Wu, X., and Zhang, G. J.: Performance of the New NCAR CAM3.5 in East Asian Summer Monsoon simulations: sensitivity to modifications of the convection scheme, J. Climate, 23, 3657–3675, doi:10.1175/2010JCLI3022.1, 2010. 23686

Ciais, P., Rayner, P., Chevallier, F., Bousquet, P., Logan, M., Peylin, P., and Ramonet, M.: Atmospheric inversions for estimating CO_2 fluxes: methods and perspectives, in: Greenhouse Gas Inventories, edited by: Jonas, M., Nahorski, Z., Nilsson, S., and Whiter, T., Springer, the Netherlands, doi:10.1007/978-94-007-1670-4_6, 69–92, 2011. 23684

Collins, W. D., Bitz, C. M., Blackmon, M. L., Bonan, G. B., Bretherton, C. S., Carton, J. A., Chang, P., Doney, S. C., Hack, J. J., Henderson, T. B., Kiehl, J. T., Large, W. G., McKenna, D. S., Santer, B. D., and Smith, R. D.: The community climate system model version 3 (CCSM3)., J. Climate, 19, 2122–2143, doi:10.1175/JCLI3761.1, 2006. 23686

Enting, I.: Inverse Problems in Atmospheric Constituent Transport, Cambridge Atmospheric and Space Science Series, Cambridge University Press, Cambridge, 2002. 23683

Gerbig, C., Lin, J. C., Wofsy, S. C., Daube, B. C., Andrews, A. E., Stephens, B. B., Bakwin, P. S., and Grainger, C. A.: Toward constraining regional-scale fluxes of CO_2 with atmospheric observations over a continent: 2. Analysis of COBRA data using a receptor-oriented framework, J. Geophys. Res.-Atmos., 108, 4757, doi:10.1029/2003jd003770, 2003. 23684, 23690, 23693

Gerbig, C., Körner, S., and Lin, J. C.: Vertical mixing in atmospheric tracer transport models: error characterization and propagation, Atmos. Chem. Phys., 8, 591–602, doi:10.5194/acp-8-591-2008, 2008. 23684, 23693

Gourdji, S. M., Mueller, K. L., Yadav, V., Huntzinger, D. N., Andrews, A. E., Trudeau, M., Petron, G., Nehrkorn, T., Eluszkiewicz, J., Henderson, J., Wen, D., Lin, J., Fischer, M., Sweeney, C., and Michalak, A. M.: North American CO_2 exchange: inter-comparison of modeled estimates with results from a fine-scale atmospheric inversion, Biogeosciences, 9, 457–475, doi:10.5194/bg-9-457-2012, 2012. 23683, 23690, 23693

Gurney, K. R., Law, R. M., Denning, A. S., Rayner, P. J., Baker, D., Bousquet, P., Bruhwiler, L., Chen, Y. H., Cials, P., Fan, S., Fung, I. Y., Gloor, M., Heimann, M., Higuchi, K., John, J., Maki, T., Maksyutov, S., Masarie, K., Peylin, P., Prather, M., Pak, B. C., Randerson, J., Sarmiento, J., Taguchi, S., Takahashi, T., and Yuen, C. W.: Towards robust regional estimates of CO_2 sources and sinks using atmospheric transport models, Nature, 415, 626–630, doi:10.1038/415626a, 2002. 23683, 23684

Hunt, B. R., Kalnay, E., Kostelich, E. J., Ott, E., Patil, D. J., Sauer, T., Szunyogh, I., Yorke, J. A., and Zimin, A. V.: Four-dimensional ensemble Kalman filtering, Tellus A, 56, 273–277, doi:10.1111/j.1600-0870.2004.00066.x, 2004. 23686, 23688

Hunt, B. R., Kostelich, E. J., and Szunyogh, I.: Efficient data assimilation for spatiotemporal chaos: a local ensemble transform Kalman filter, Physica D, 230, 112–126, doi:10.1016/j.physd.2006.11.008, 2007. 23685, 23686, 23687, 23688

Huntzinger, D. N., Gourdji, S. M., Mueller, K. L., and Michalak, A. M.: The utility of continuous atmospheric measurements for identifying biospheric CO_2 flux variability, J. Geophys. Res.-Atmos., 116, D06110, doi:10.1029/2010JD015048, 2011. 23689

Huntzinger, D., Post, W., Wei, Y., Michalak, A., West, T., Jacobson, A., Baker, I., Chen, J., Davis, K., Hayes, D., Hoffman, F., Jain, A., Liu, S., McGuire, A., Neilson, R., Potter, C., Poulter, B., Price, D., Raczka, B., Tian, H., Thornton, P., Tomelleri, E., Viovy, N., Xiao, J., Yuan, W., Zeng, N., Zhao, M., and Cook, R.: North American Carbon Program (NACP) regional interim synthesis: terrestrial biospheric model intercomparison, Ecol. Model., 232, 144–157, doi:10.1016/j.ecolmodel.2012.02.004, 2012. 23683

Kanamitsu, M., Ebisuzaki, W., Woollen, J., Yang, S.-K., Hnilo, J. J., Fiorino, M., and Potter, G. L.: NCEP–DOE AMIP-II reanalysis (R-2), B. Am. Meteorol. Soc., 83, 1631–1643, doi:10.1175/BAMS-83-11-1631, 2002. 23687

Kitanidis, P. K.: Introduction to Geostatistics: Applications in Hydrogeology, Stanford-Cambridge program, Cambridge University Press, Cambridge, 1997. 23688

Kretschmer, R., Gerbig, C., Karstens, U., and Koch, F.-T.: Error characterization of CO_2 vertical mixing in the atmospheric transport model WRF-VPRM, Atmos. Chem. Phys., 12, 2441–2458, doi:10.5194/acp-12-2441-2012, 2012. 23684, 23693

Kretschmer, R., Gerbig, C., Karstens, U., Biavati, G., Vermeulen, A., Vogel, F., Hammer, S., and Totsche, K. U.: Impact of optimized mixing heights on simulated regional atmospheric transport of CO_2, Atmos. Chem. Phys., 14, 7149–7172, doi:10.5194/acp-14-7149-2014, 2014. 23684

Lauvaux, T., Pannekoucke, O., Sarrat, C., Chevallier, F., Ciais, P., Noilhan, J., and Rayner, P. J.: Structure of the transport uncertainty in mesoscale inversions of CO_2 sources and sinks using ensemble model simulations, Biogeosciences, 6, 1089–1102, doi:10.5194/bg-6-1089-2009, 2009. 23684

Li, H., Kalnay, E., and Miyoshi, T.: Simultaneous estimation of covariance inflation and observation errors within an ensemble Kalman filter, Q. J. Roy. Meteor. Soc., 135, 523–533, doi:10.1002/qj.371, 2009. 23687, 23688

Lin, J. C. and Gerbig, C.: Accounting for the effect of transport errors on tracer inversions, Geophys. Res. Lett., 32, L01802, doi:10.1029/2004GL021127, 2005. 23684, 23693

Liu, J., Fung, I., Kalnay, E., and Kang, J.-S.: CO_2 transport uncertainties from the uncertainties in meteorological fields, Geophys. Res. Lett., 38, L12808, doi:10.1029/2011GL047213, 2011. 23685, 23687, 23688, 23693

Liu, J., Fung, I., Kalnay, E., Kang, J.-S., Olsen, E. T., and Chen, L.: Simultaneous assimilation of AIRS XCO_2 and meteorological observations in a carbon climate model with an ensemble Kalman filter, J. Geophys. Res.-Atmos., 117, D05309, doi:10.1029/2011JD016642, 2012. 23685, 23687

Michalak, A., Bruhwiler, L., and Tans, P.: A geostatistical approach to surface flux estimation of atmospheric trace gases, J. Geophys. Res.-Atmos., 109, D14109, doi:10.1029/2003JD004422, 2004. 23683

Michalak, A. M., Hirsch, A., Bruhwiler, L., Gurney, K. R., Peters, W., and Tans, P. P.: Maximum likelihood estimation of covariance parameters for Bayesian atmospheric trace gas surface flux inversions, J. Geophys. Res.-Atmos., 110, D24107, doi:10.1029/2005JD005970, 2005. 23684

Miyoshi, T.: The Gaussian approach to adaptive covariance inflation and its implementation with the local ensemble transform Kalman filter, Mon. Weather Rev., 139, 1519–1535, doi:10.1175/2010MWR3570.1, 2011. 23687, 23688

Oleson, K. W., Niu, G.-Y., Yang, Z.-L., Lawrence, D. M., Thornton, P. E., Lawrence, P. J., Stöckli, R., Dickinson, R. E., Bonan, G. B., Levis, S., Dai, A., and Qian, T.: Improvements to the Community Land Model and their impact on the hydrological cycle, J. Geophys. Res.-Biogeo., 113, G01021, doi:10.1029/2007JG000563, 2008. 23686

Parazoo, N. C., Denning, A. S., Kawa, S. R., Pawson, S., and Lokupitiya, R.: CO_2 flux estimation errors associated with moist atmospheric processes, Atmos. Chem. Phys., 12, 6405–6416, doi:10.5194/acp-12-6405-2012, 2012. 23684

Peters, W., Jacobson, A. R., Sweeney, C., Andrews, A. E., Conway, T. J., Masarie, K., Miller, J. B., Bruhwiler, L. M. P., Petron, G., Hirsch, A. I., Worthy, D. E. J., Werf, G. R. v. d., Randerson, J. T., Wennberg, P. O., Krol, M. C., and Tans, P. P.: An atmospheric perspective on North American carbon dioxide exchange: CarbonTracker, Proceedings of the National Academy of Sciences, with updates documented at: http://carbontracker.noaa.gov (last access: 12 September 2014), 104, 18925–18930, doi:10.1073/pnas.0708986104, 2007. 23683, 23688, 23689, 23693, 23694

Pino, D., Vilà-Guerau de Arellano, J., Peters, W., Schröter, J., van Heerwaarden, C. C., and Krol, M. C.: A conceptual framework to quantify the influence of convective boundary layer development on carbon dioxide mixing ratios, Atmos. Chem. Phys., 12, 2969–2985, doi:10.5194/acp-12-2969-2012, 2012. 23684

Raczka, B. M., Davis, K. J., Huntzinger, D., Neilson, R. P., Poulter, B., Richardson, A. D., Xiao, J., Baker, I., Ciais, P., Keenan, T. F., Law, B., Post, W. M., Ricciuto, D., Schaefer, K., Tian, H., Tomelleri, E., Verbeeck, H., and Viovy, N.: Evaluation of continental carbon cycle simulations with North American flux tower observations, Ecol. Monogr., 83, 531–556, doi:10.1890/12-0893.1, 2013. 23683

Schuh, A. E., Denning, A. S., Corbin, K. D., Baker, I. T., Uliasz, M., Parazoo, N., Andrews, A. E., and Worthy, D. E. J.: A regional high-resolution carbon flux inversion of North America for 2004, Biogeosciences, 7, 1625–1644, doi:10.5194/bg-7-1625-2010, 2010. 23693

Sheskin, D.: Handbook of Parametric and Nonparametric Statistical Procedures, 3 edn., Taylor and Francis, Boca Raton, Florida, 2003. 23689

Stephens, B. B., Gurney, K. R., Tans, P. P., Sweeney, C., Peters, W., Bruhwiler, L., Ciais, P., Ramonet, M., Bousquet, P., Nakazawa, T., Aoki, S., Machida, T., Inoue, G., Vinnichenko, N., Lloyd, J., Jordan, A., Heimann, M., Shibistova, O., Langenfelds, R. L., Steele, L. P., Francey, R. J., and Denning, A. S.: Weak northern and strong tropical land carbon uptake from vertical profiles of atmospheric CO_2, Science, 316, 1732–1735, doi:10.1126/science.1137004, 2007. 23684

Tarantola, A.: Inverse Problem Theory and Methods for Model Parameter Estimation, Society for Industrial and Applied Mathematics, Philadelphia, 2005. 23683

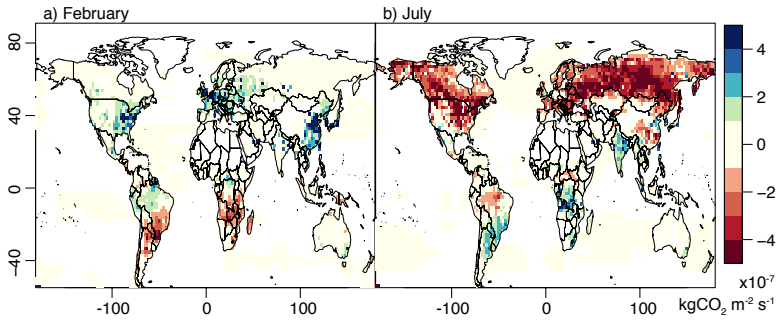

Figure 1. Average CT CO_2 fluxes (version 2011oi) for **(a)** Feburary and **(b)** July 2009. The fluxes include biosphere, ocean, fossil fuel, and biomass burning fluxes (http://www.esrl.noaa.gov/gmd/ccgg/carbontracker/CT2011_oi).

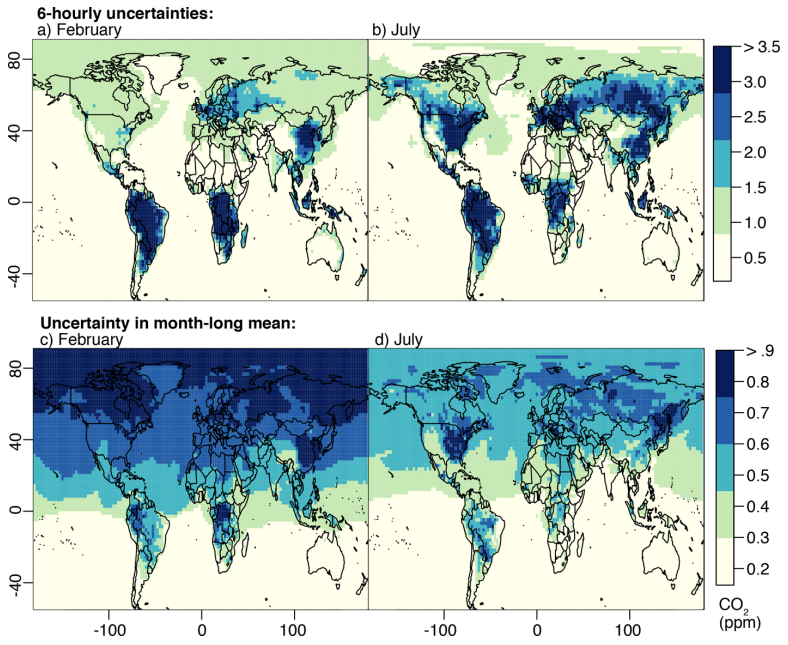

Figure 2. The top panels display average 6 hourly CO_2 transport uncertainties estimated by CAM–LETKF. The uncertainties (standard deviations) are for the surface model layer for **(a)** February and **(b)** July 2009. To create these plots, we calculate the ensemble variance at each time step and subsequently average the variances across all time steps. These standard deviations are the square root these meaned 6 hourly variances. Furthermore, these plots include model output from all 24 h of each day. The Supplement provides analogous figures for daytime- or nighttime-only model output. The bottom-panels (**c** and **d**), in contrast, display the standard deviation in month-long averaged surface CO_2 concentrations.

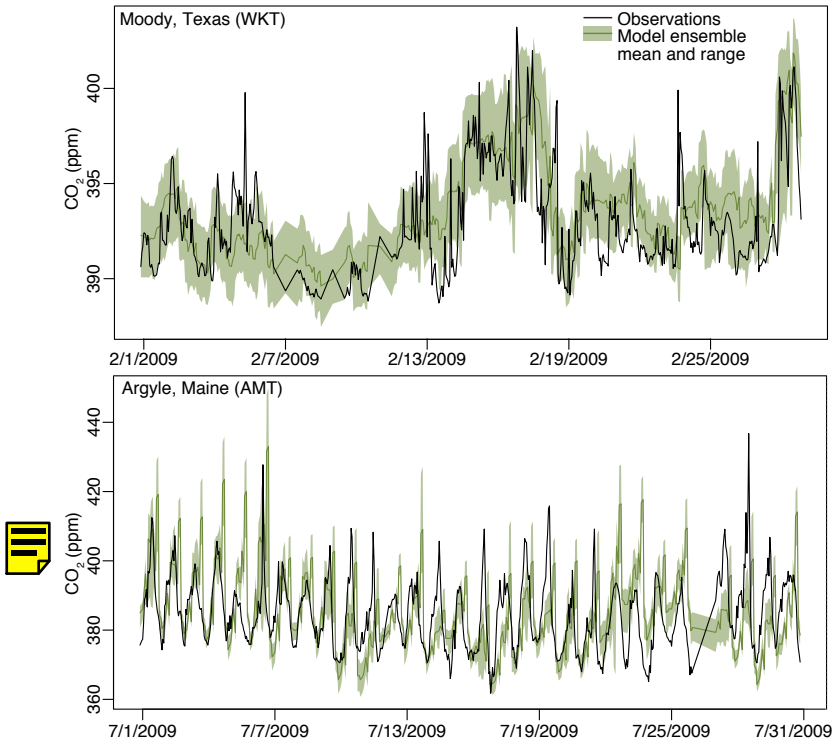

Figure 3. Hourly averaged measured CO_2 at **(a)** Moody, Texas, and **(b)** Argyle, Maine, compared against the CAM–LETKF model ensemble. Measurements are from the top inlet height at each location. In this figure, the model ensemble represents uncertainties due to atmospheric transport but not other errors (e.g., due to the fluxes, model resolution, etc.).

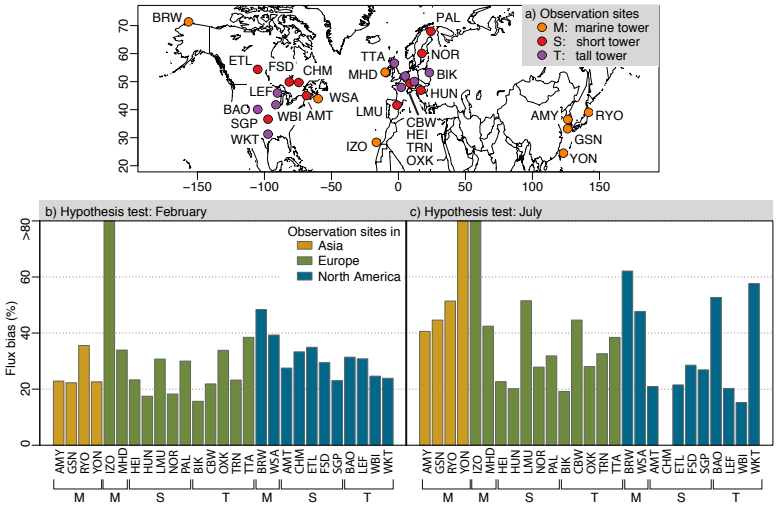

Figure 4. Results of the hypothesis test (Sects. 2.4 and 3.3) at a selection of global CO_2 observation sites. Panel **(a)** shows the location, name, and type of each observation site examined in the hypothesis test. At sites with multiple measurement or inlet heights, we model the top inlet. Panels **(b)** and **(c)** show the test results for February and July 2009. The test asks the following question: how biased would CT fluxes need to be before CO_2 observation sites would detect that bias above the estimated CO_2 transport uncertainties?

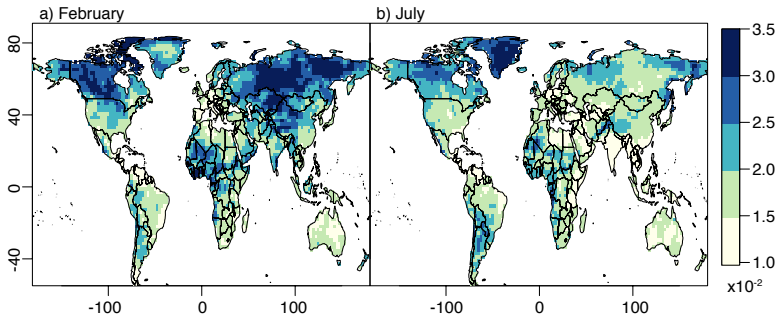

Figure 5. The coefficient of variation (CV, unitless) for the monthly-averaged model surface layer. The results plotted here are for the synthetic tracer simulation (Sects. 2.5 and 3.4). In that simulation, the synthetic fluxes have a constant spatial distribution. The resulting CV (σ/μ) shows the distribution of month-long, surface-level transport uncertainties independent of the spatial distribution in the fluxes. Note that this plot displays the results from land regions only.

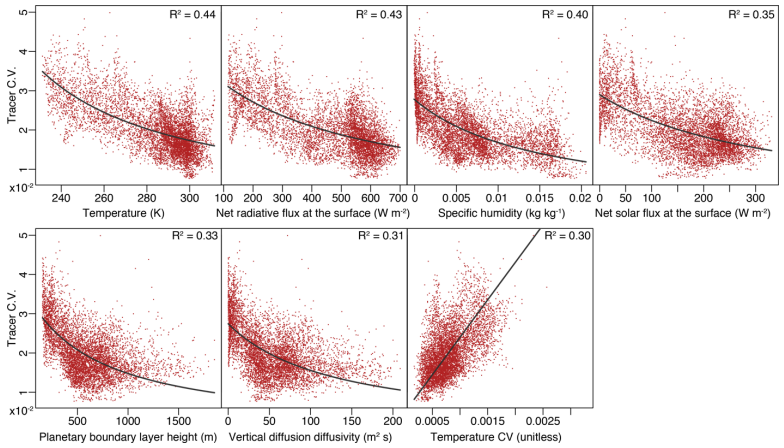

Figure 6. Each panel shows the correlation between the synthetic tracer CV (Fig. 5) and various monthly-averaged meteorological parameters estimated by CAM-LETKF. We test the correlation with 60 different parameters (Table S2) and plot the relationships for which $R^2 \geq 0.3$. In all cases, we fit both a standard major axis regression and nonlinear least squares $\left(\frac{1}{[\beta_1 \times \text{parameter} + \beta_2]}\right)$ and plot the regression with the higher correlation coefficient.